fluids

MDPI

Article

Thermodynamics Characterization of Lung Carcinoma, Entropic Study and Metabolic Correlations

Francesco Farsaci [1], Ester Tellone [2,*], Antonio Galtieri [2] and Silvana Ficarra [2]

[1] Institute for Chemical and Physical Processes (IPCF-C.N.R.), Via Ferdinando Stagno d'Alcontres 37, Faro Superiore, 98158 Messina, Italy; farsaci@me.cnr.it

[2] Department of Chemical, Biological, Pharmaceutical and Environmental Sciences, University of Messina, Viale Ferdinando Stagno d'Alcontres 31, 98166 Messina, Italy; agaltieri@unime.it (A.G.); sficarra@unime.it (S.F.)

* Correspondence: etellone@unime.it

Received: 3 July 2020; Accepted: 31 August 2020; Published: 26 September 2020

Abstract: In recent years, the use of dielectric spectroscopy as an investigation technique to determine the chemical–physical characteristics of biological materials has had a great increase. This study used the non-equilibrium thermodynamics with internal variables theory to test the potential pathological features of lung cancer. After a brief exploration of the dielectric polarization concept highlighting some aspects that were used, some thermodynamic functions were obtained as functions of the frequency, both for lung tumor cells and physiological ones. Variations in the intensity of values but not in the trend of the curves were observed and this was attributed to the perturbing field. The trend of this field explains the behavior of phenomena described by other functions, as related to the frequencies of the perturbing field. Compared to the physiological ones, the cancer cells appeared to be "more predisposed" to conserve their state as characterized by minor entropy production, probably because this helped cells to obtain the required adenosine triphosphate (ATP) from the minimum amount of nutrients.

Keywords: non-equilibrium thermodynamics; lung carcinoma

1. Introduction

As a leading cause of death in industrialized countries, lung cancer is considered one of the most aggressive cancers [1,2]. Smoking remains the major risk factor for this type of cancer genetic factors may contribute to 10-15% of the causes. It is possible to make some distinction between small and non-small cell carcinoma, and these categories help to determine a different prognosis and treatment of the disease. Correctly staging lung cancer is important because to date, one of the main therapeutic objectives of cancer medicine is early diagnosis. Cancer screening programs have been shown to save many lives and increase survival, along with the support of several antiproliferative studies [3,4]. It is clear, therefore, that timely diagnosis is the most powerful weapon of public health against all cancers in general. To achieve this goal, however, it is necessary to have adequate and sophisticated highly sensitive diagnostic techniques, possibly non-invasive and inexpensive. Various techniques are currently used for this purpose such as computed tomography (CT), positron emission tomography (PET), and magnetic resonance imaging (MRI) which can obtain high-definition "images" of the whole organism or part of it. However, even today it is difficult to detect the first signs of an oncological alteration. This is due to both the indistinguishable characteristics of the first cancer cells, as well as the difficulty in coordinating non-invasive and low

costs screening with diagnostic sensitivity. In recent years there has been a rising interest in dielectric spectroscopy, an investigation technique that can obtain information on the chemical–physical characteristics of biological materials starting from the dielectric properties [5–23]. The response of biological tissues to an electric field is characterized by two intrinsic properties conductivity and relative permittivity, which are both dependent on frequency. In particular, conductivity is related to the capability of the tissue to be crossed by an electric field, and permittivity is related to material's ability to store energy, and both may provide important information about the studied matter [24–26]. Sugitani et al. (2014) found considerable diversity in the complex permittivity of breast tumor tissue in several studies using probes to detect small changes in dielectric properties caused by cancer invasiveness evidenced changes in permittivity and conductivity as tissue transformed from normal to cancerous [27–29]. In this contest text, the development of probes using this technique provided wide versatility accompanied by easy application, low invasiveness and low cost. The present study attempted to find improvements in the diagnosis and treatment of lung carcinoma, making use of complex mathematical techniques leading to the formulation of new dielectric entities capable of providing new biological information about cancer cells.

2. Methods

This paper referred to the experimental data by Wang et al. [7], in which 109 patients including 71 males and 38 females aged 61.41 ± 9.96 years who had undergone removal of cancerous lung tissue, were studied. The mean and standard deviation of relative permittivity, conductivity (our starting point values) and relaxation times, were measured [7]. The approach we used in the present paper was theoretical, and the thermodynamic functions introduced in the Appendix A were calculated for healthy and cancerous lung tissue, correlating the obtained data with the dielectric measurements.

Polarization Vector

Some continuum electrodynamics concepts are detailed below before our results are described and some phenomena are explained. Placing $\underline{r}_q$ and $\underline{r}_{-q}$ as vectors position of the +q and -q charges with respect to a O point, P_{dip} is indicated as dipole moment with respect to O:

$$\underline{P}_{dip} = q\underline{r}_q + (-q)\underline{r}_{-q}$$

By choosing as O the barycentre of the charge (-q) we have $\underline{r}_q = r$ and $\underline{r}_{-q} = 0$. Thus the dipole moment becomes:

$$\underline{P}_{dip} = q\underline{r} \quad (1)$$

If N dipoles are contained in volume V, the vector denoted by $\underline{P}$ is called the moment of electric dipole moment per unit of volume (or polarization vector):

$$\underline{P} = \frac{\sum_{i=1}^{N} \underline{P}_i}{V} \quad (2)$$

where $\underline{P}_i$ is the dipole moment of the i-th dipole.

That is, the dipole moment per unit of volume is the vector sum of the N dipoles divided by the volume V that contains them. Considering a material system in a region of space with an electric field, it will be perturbed by the field generating dipoles inside it or the realigning of any existing dipoles, whose moment is $\underline{P}$. It is shown that the presence of matter (with dipoles) is equivalent to a new distribution of charges of ρ' density of volume and σ' surface as that:

$$\rho' = -div\,\underline{P} \quad (3)$$

$$\sigma' = \underline{P} \cdot \underline{n} \tag{4}$$

where $\underline{n}$ is the surface normal. Recalling that $\underline{P} = \underline{P}^{(0)} + \underline{P}^{(1)}$ this applies to $P^{(0)}$ and $P^{(1)}$ with some clarifications related to their meaning ($\underline{P}^{(0)}$ and $\underline{P}^{(1)}$ are both polarization vectors, one is associated with deformation and the other with orientation). As cancer cells are biological materials and strongly polar, their study will therefore be addressed by evaluating $\underline{P}^{(1)}$ associated with the orientation polarization that can provide important information. Regardless of frequency, the qualitative differences relating to phenomena in healthy and cancerous cells were studied first in this work. This is because, at any frequency, the curves that characterize healthy cells are different from cancerous ones only in intensity, not in shape. A qualitative, not quantitative, analysis was therefore made. Dielectric experimental data in this paper refer to the studies of Wang et al. (2014) [7].

3. Results

The development of our study started from relative permittivity ε_r, conductivity c and relaxation times for cancerous ($\sigma = 6.8 \times 10^{-7}$s) and healthy ($\sigma = 5.7 \times 10^{-7}$s) cells respectively [7]. Figure 1 shows that $P_t^{(1)}$ for cancer cells was lower than for healthy $P_f^{(1)}$; and for each frequency:

$$P_t^{(1)} < P_f^{(1)} \tag{5}$$

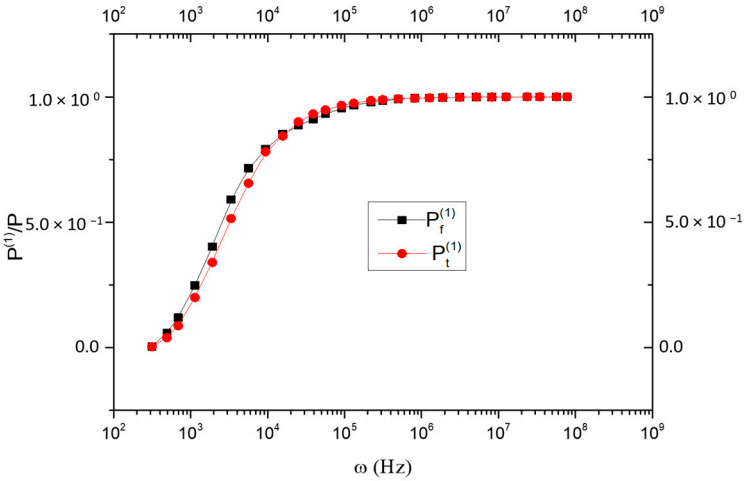

Figure 1. Comparison between normal (black line) and cancerous cells (red line) orientation polarization $P^{(1)}$ values as a function of frequency, see equation (A23).

Recalling (4), we say that the surface charge density in cancerous was lower than in healthy cells; it follows that cancerous cells possess fewer charges per unit area than healthy cells. Cancerous cells occupy a larger volume than healthy ones, they have a negative charge, but they have no fewer charges in total, they have fewer charges per unit area. Figure 2 describes the polarization of a cell immersed in an electric field $\underline{E}$. Since there is a large prevalence of phenomena related to orientation polarization:

$$P' = \tilde{\sigma} \tag{6}$$

with $\tilde{\sigma}$ as the surface density. The displacement phenomena (currents and conductivity) associated with polarization phenomena by orientation are greater in cancer at every frequency (see Figures 2 and 3). This can be explained by Figure 4 and recalling that:

$$dP^{(1)}/dt = L^{(1)}E^{(1)} \tag{7}$$

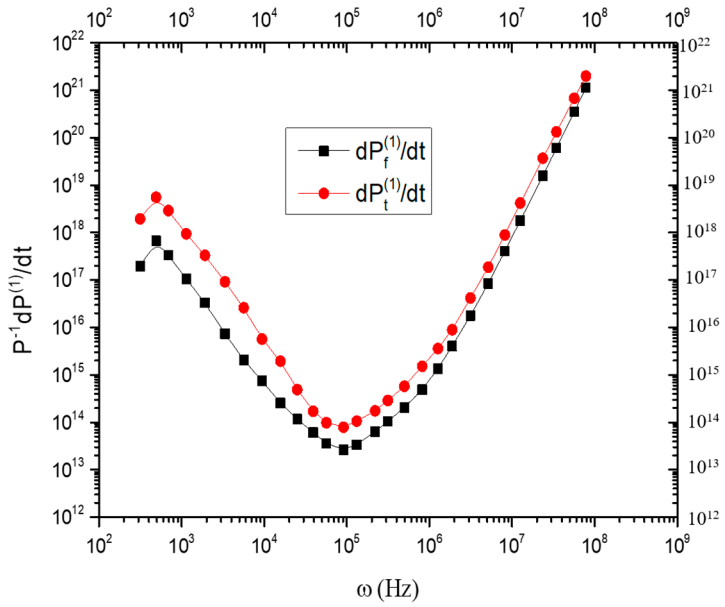

Figure 2. Comparison between normal (black line) and cancerous cells (red line) of the displacement current as a function of frequency, see Equations (A6), (A8) and (A16).

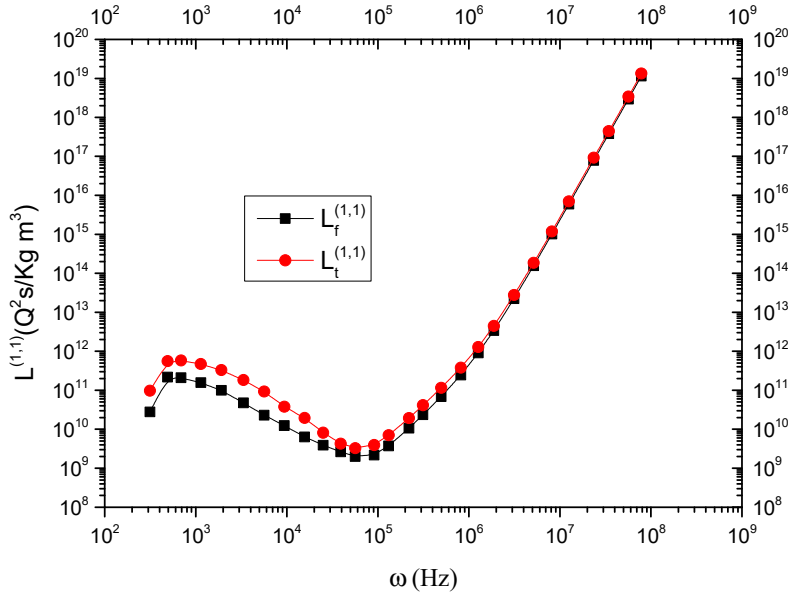

Figure 3. Comparison between normal (black line) and cancerous cells (red line) of displacement conductivity $L^{(1,1)}$as a function of frequency, see Equation (A17).

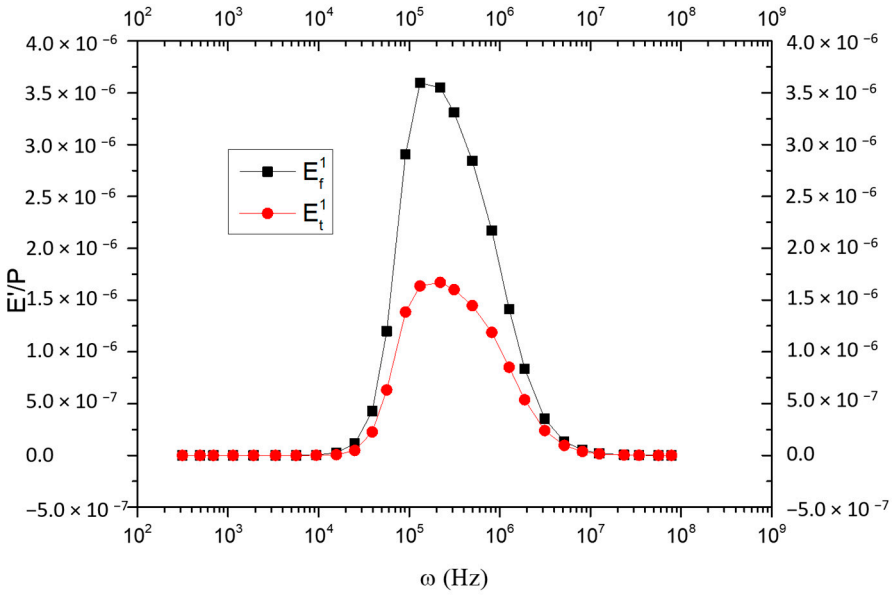

Figure 4. Comparison between normal (black line) and cancerous cells (red line) of the field $E^{(1)}$ as a function of the frequency of perturbation, see Equation (A6).

In fact, Figure 4 shows that $E_t^{(1)}<E_f^{(1)}$, i.e., the field generated by the dipoles stimulated by a harmonic perturbation was smaller in cancerous cells and it was opposed to the disturbing field. Then, the latter is less inhibited in cancerous than in healthy cells, and this happens at the same frequency but with different intensity (curves show the same shape). This implies an increase in currents and displacement conductivity in cancerous cells (see Figures 2 and 3). From Figure 5:

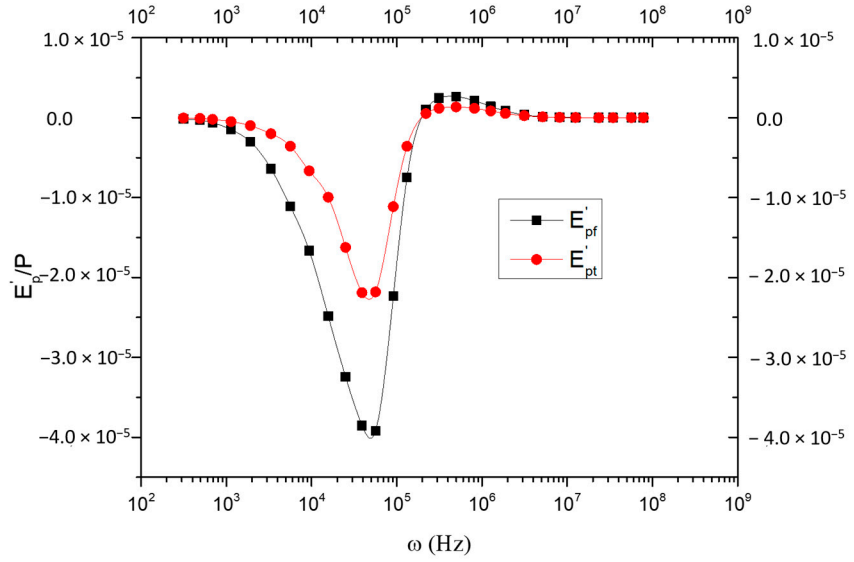

Figure 5. Comparison between normal (black line) and cancerous cells (red line) of the field $E_{P(1)}^{(1)}$ associated with the polarization $P^{(1)}$ as a function of frequency, see Equation (A8).

$$E_p^{(1)} = (a^{(00)}\text{-}a^{(11)})\, P^{(1)}$$

we note that:

$$E_{pt}^{(1)} > E_{pf}^{(1)}$$

It could be argued that $P_p^{(1)} < P_f^{(1)}$ should result in $E_{pt}^{(1)} < E_{pf}^{(1)}$. However, an important role is played by the ($a^{(00)} - a^{(11)}$) terms as can be seen from Figure 6. In fact, $P^{(1)}$ is related only to polarization by orientation (according to Debye's scheme), but $a^{(00)}$ and $a^{(11)}$ are linked to intrinsic characteristics of the medium related to other phenomena. From Figure 7, which shows the trend of entropy production, it is possible to observe that healthy cells have greater entropy than cancerous ones. This means that cancer is a more orderly system than a physiological one, as already found in other pathologies. However, the temporal evolution of tumor pathogenesis is not the object of this study, because the results reported here are derived only from the measurements reported in reference [7]. These results, obtained by processing the experimental data of Wang et al. (2014), allowed us to achieve a new characterization of lung cancer by highlighting several peculiarities of cancer at the time of the dielectric measurement [7]. The obtained curves will be now analyzed as a function of frequency. In the frequency range considered, two sectors are identified in which the trend of the curve is oppositional. The frequency separating the two sections is about $\omega = 10^5$ Hz (see Figures 1 and 6).

$$A = [\omega \mid \omega < 10^5 \text{ Hz}]$$

$$B = [\omega \mid \omega \geq 10^5 \text{ Hz}]$$

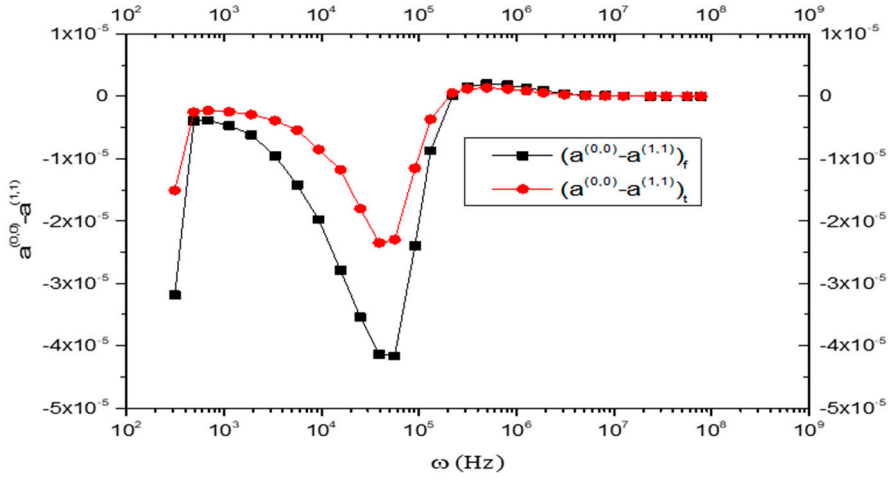

Figure 6. Comparison between the difference of state coefficients $a^{(0,0)}$ and $a^{(1,1)}$ in normal (black line) and cancerous cells (red line) as a function of frequency, see Equations (A15) and (A16).

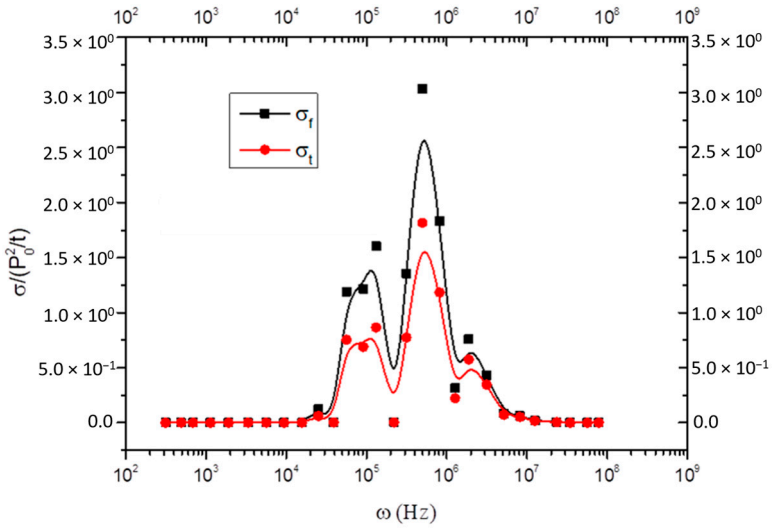

Figure 7. Comparison between normal (black line) and cancerous cells (red line) of the trend of entropy production as a function of frequency perturbation, see Equation (A24).

Section for $\omega < 10^5$ Hz

Figure 1 shows an increase in $P^{(1)}$ value as ω increases for both cancerous and healthy cells. Therefore, there is a dipole moment that increases with increasing frequency along with the surface charge density. Smaller and smaller dipoles are set in motion in both cell types, but in cancer at slightly higher frequencies, $P_t^{(1)}$ had values equal to $P_f^{(1)}$ This could mean that in cancer, dipoles are less "massive" or "smaller" and therefore they begin to oscillate at higher frequencies. Or more likely, the dipoles number could be fewer per volume unit. In fact, phenomena that neutralize a certain number of dipoles can occur in cancer (this could be due to the assembly of platelets). Figure 2 shows a decrease in the displacement current $dP^{(1)}/dt$ linked to $P^{(1)}$ value as the frequency increases. Since $P^{(1)}$ value increased, i.e., the dipole moment per unit of volume increased, it is to be expected that the temporal variation decreases. This is due to the fact that the number of dipoles per unit of volume increases and therefore there is a greater "inertia" per unit of volume. $P_t^{(1)} < P_f^{(1)}$ indicates a lower "inertia" for cancerous compared to healthy cells and therefore $dP_t^{(1)}/dt > dP_f^{(1)}/dt$, as shown in Figure 2. A similar discussion can be made for the $L^{(11)}$ displacement conductivity values shown in Figure 3. Additionally, in this case, there was a decrease in $L^{(11)}$ value as ω increased and the previous considerations are valid. Figure 4, as the frequency increases, shows an increase in the electric field associated with $dP^{(1)}/dt$ displacement currents.

Recalling that $E_p^{(1)} = (a^{(00)} - a^{(11)})\, P^{(11)}$, the field by which the $P^{(1)}$ value was generated is less and less propagated since the characteristics of the medium identified by the difference $(a^{(00)} - a^{(11)})$ prevent its propagation (see Figure 5), even if the $P^{(1)}$ value increases with frequency. It should be noted that the $E_p^{(1)}$ field was negative. This is correct because it was generated by dipoles that oppose the disturbing field, thus generating an opposite field. As already mentioned, the $E_p^{(1)}$ field is greater in cancer because the difference $(a^{(00)} - a^{(11)})$ was greater in cancerous than in healthy cells. Figure 6 shows that $a^{(11)} > a^{(00)}$, therefore anelastic phenomena were more evident than elastic in the medium. In particular, it is:

$$a_t^{(00)} - a_t^{(11)} > a_f^{(00)} - a_f^{(11)} \quad (8)$$

$$a_t^{(00)} - a_f^{(00)} > a_t^{(11)} - a_f^{(11)} \quad (9)$$

The latter shows in cancerous and healthy cells, a greater difference between the elastic characteristics than the anelastic ones. In other words, the elastic characteristics varied more than the anelastic ones between cancerous and healthy cells. Therefore, from Figures 8 and 9 $a_f^{(00)} > a_t^{(00)}$ and $a_f^{(11)} > a_t^{(11)}$, both the elastic characteristics $(a^{(11)})$ and the anelastic ones were greater in the healthy cells compared to the cancerous ones. Figure 7 shows lower entropy production values in cancer, then cancer tissue has a greater "order" than healthy cells.

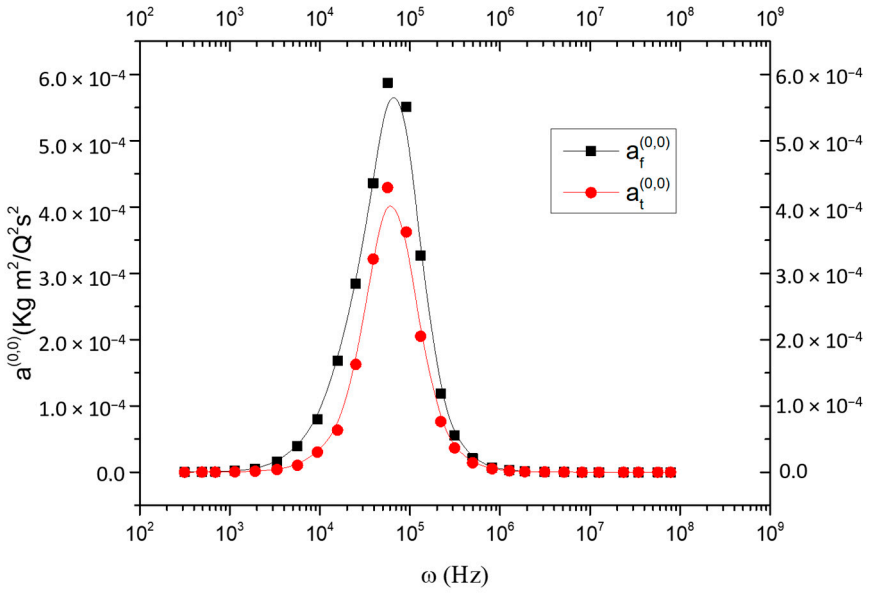

Figure 8. Comparison between normal (black line) and cancerous cells (red line) of state coefficients $a^{(0,0)}$ as a function of frequency, see Equation (A15).

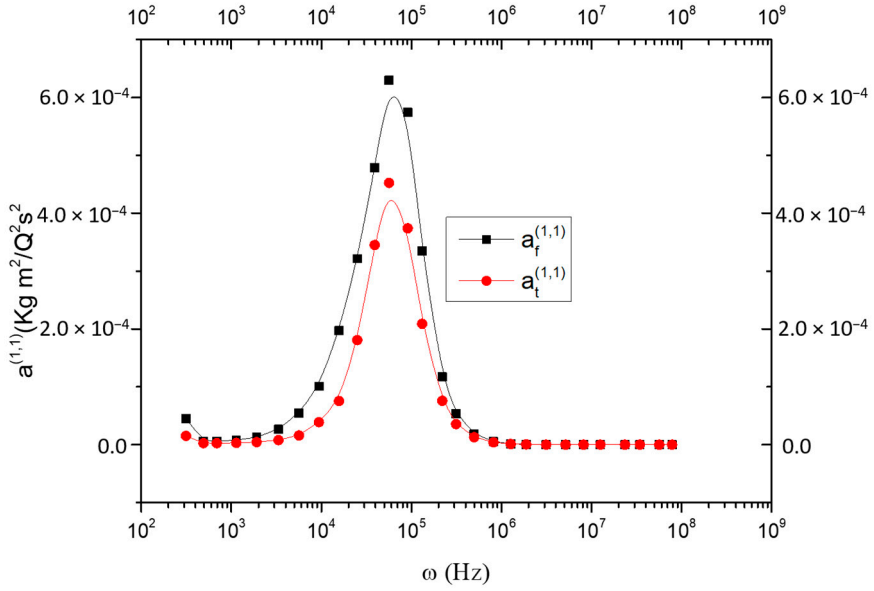

Figure 9. Comparison between normal (black line) and cancerous cells (red line) state coefficients $a^{(1,1)}$ as a function of frequency, see Equation (A16).

Section for ω > 10⁵ Hz

Figure 1 shows almost constant $P^{(1)}$ values; i.e., the dipole moment per volume unit and the surface charge density were constant (or almost): from 10^5 Hz onwards, the dipole moments per volume unit did not follow the speed with which varies the field, both for cancerous and healthy cells. With this in mind, stabilizing "inertia" per unit of volume increases its temporal variation prevented earlier by a continuous increase in it. As soon as the $P^{(1)}$ value stabilizes, $dP^{(1)}/dt$ starts growing again.

As said before, if $P_t^{(1)}<P_f^{(1)}$ and therefore the $P_t^{(1)}$ value has a "lower inertia", its temporal variation, corresponding to the displacement current, will be greater as shown in Figure 2. After reaching the minimum at a frequency of about $\omega = 10^5$ Hz, the $dP^{(1)}/dt$ displacement current tended to increase both in cancerous and in healthy cells (see Figure 2). The same speech is for the $L^{(11)}$

displacement conductivity values shown in Figure 3. After reaching a minimum value around ω = 10^5 Hz the displacement conductivity tended to rise with $L_t^{(11)} > L_f^{(11)}$. Additionally, in Figure 4, there is a decrease in the electric field $E^{(1)}$. Figure 5 shows $E_p^{(1)}$ values increasing and stabilizing for ω greater than 10^6 Hz with $E_{pt}^{(1)} > E_{pf}^{(1)}$. This is linked to the increase of ($a^{(00)} - a^{(11)}$) which assumed almost constant values in the same range in which $E_p^{(1)}$ values were stabilized (see Figure 5). Additionally, in this case, the considerations made on $a^{(00)} - a^{(11)}$ in section A are valid. In Figures 6, 8 and 9, the valuations made in section A are valid. In particular, the values of $a^{(00)}$ and $a^{(11)}$ increased up to a maximum of around 10^5 Hz and then decreased, keeping constant for ω > 10^6 Hz. Here, too, the relationships (8) and (9) are valid. Figure 7 shows a greater production of entropy in healthy than in cancerous cells. The value reached a maximum between 10^5 and 10^6 Hz and then decreased and almost cancelled for ω > 10^7 Hz. However, even in this section, cancerous cells show a greater "order" than healthy ones.

4. Conclusions

The thermodynamic study of the relaxation phenomena conducted on lung cancer shows phenomena related to orientation polarization $P^{(1)}$, displacement currents $dP^{(1)}/dt$, displacement conductivity $L^{(11)}$ are very similar for both cancer and physiological tissues, except for the intensity with the variation of the perturbation frequency. The present analysis identified the cause of the different intensity in field $E^{(1)}$, generated by the dipoles stimulated by the harmonic perturbation; in detail, when stimulated by a harmonic perturbation, the already existing and generating dipoles produce a field opposed to the disturbing field which is of lesser intensity in the cancerous tissue than in the physiological one (see Figures 2–4). What was observed is attributable to the tendency of cancerous cells to be more depolarized than their normal counterparts [30]. In addition, the membrane depolarization seems to be closely linked to the invasiveness of the cancerous cells as recently demonstrated by Lobikin et al., 2012 [31]. Another important conclusion derives from the evaluation of the entropy production trend (see Figure 7); cancer is a thermodynamically more ordered tissue than a physiological one. It is good to remember that this result has already been found in other types of pathologies [6,11]. The tumor seems to be "more predisposed" to conserve its state characterized by minor entropy production compared to the physiological one, thus showing a greater opposition to everything that tries to change its state, as, for example, a potential treatment of the pathology. The low rate of entropy production in some metabolic situations could be an advantage for cancerous cells. In fact, the rapid growth of the tumor mass is not always accompanied by an efficient blood supply. This leads to greater difficulty for highly proliferative cells to find nutrients than for normal cells. In this case, the cancerous cells, maintaining a stationary state characterized by the minimum rate of entropy production, are able to supply the required ATP from the minimum amount of nutrients. This condition could be related to the paradox of the "Warburg effect" shown by some growing cancerous cells, characterized by a metabolic slowdown even when oxygen is plentiful [32,33]. In this case, the energy requirement is guaranteed by the use of glucose-6-phosphate (G6P) in the two metabolic fluxes: anaerobic glycolysis, which produces ATP; and Pentose Phosphate Pathway (PPP), which produces reducing power (NADPH)-required co-factor for reductive biosynthesis as well as for the maintenance of the cellular redox state, and pentose phosphate building blocks of nucleotide structures. The "metabolic silencing" of an indispensable organelle such as a mitochondrion, with the scarce or reduced use of oxygen, and the lack of both carbon dioxide production and partially reduced oxygen products (ROS), would justify the low entropy observed. Furthermore, the lack of decarboxylation processes (typical of the Krebs cycle) and of the complete oxidation of the pyruvate would save the carbon structures necessary for biosynthetic processes. In simple words, the "energy sacrifice" is imposed by maintaining an adequate entropic state for the neoplastic tissue and becomes optimal for its growth.

Author Contributions: Conceptualization: F.F. and E.T.; Methodology: F.F. and E.T.; Formal analysis: F.F.; Validation: S.F. and A.G. All authors have read and agreed to the published version of the manuscript.

Funding: This research received no external funding.

Conflicts of Interest: The authors declare no conflict of interest.

Abbreviations

ATP: Adenosine Triphosphate
CT: Computed Tomography
PET: Positron Emission Tomography
MRI: Magnetic Resonance Imaging
G6P: Glucose-6-Phosphate
PPP: Pentose Phosphate Pathway
ROS: Reduced Oxygen Products

Appendix A

Kluitenberg's theory is based on the idea that the usual variables of non equilibrium thermodynamics are insufficient to describe some phenomena that occur in a medium when it is subject to perturbation. In particular they are insufficient to describe relaxation dielectric phenomena in a continuous media (we neglect magnetic effects).

It is assumed that the specific entropy s of an elastic dielectric is a function of the specific internal energy u, the specific polarization $\underline{p}$ and and $\underline{p}^{(1)}$:

$$s = s\left(u\left|\underline{p}\right|\underline{p}^{(1)}\right) \tag{A1}$$

where the following decomposition is obtained

$$\underline{p} = \underline{p}^{(0)} + \underline{p}^{(1)} \tag{A2}$$

here, in the Debye's model, $p^{(0)}$ is deformation polarization and $p^{(1)}$ is orientation polarization.

From this it follows [10,34–36]:

$$\begin{cases} \dfrac{1}{T} = \dfrac{\partial s\left(u.\underline{p}, \underline{p}^{(1)}\right)}{\partial u} \\ \underline{E}^{(eq)} = -T\dfrac{\partial s\left(u.\underline{p}, \underline{p}^{(1)}\right)}{\partial \underline{p}} \\ \underline{E}^{(1)} = T\dfrac{\partial s\left(u.\underline{p}, \underline{p}^{(1)}\right)}{\partial \underline{p}^{(1)}} \end{cases} \tag{A3}$$

Moreover it is introduced the vector $\underline{E}^{(ir)}$ defined as:

$$\underline{E}^{(ir)} = \underline{E} - \underline{E}^{(eq)} \tag{A4}$$

where $\underline{E}$ is the electric field which occurs in Maxwell's equations. The vector $\underline{E}^{(ir)}$ is the irreversible electric field. It can be shown the following phenomenological equation [10,34–36]:

$$\underline{E}^{(ir)} = L^{(0,0)}\frac{d\underline{p}}{dt} \tag{A5}$$

$$\frac{d\underline{p}^{(1)}}{dt} = +L^{(1,1)}\underline{E}^{(1)} \tag{A6}$$

$$\underline{E}^{(eq)} = a^{(0,0)}\left(\underline{P} - \underline{P}^{(1)}\right) = a^{(0,0)}\underline{P}^{(0)} \tag{A7}$$

$$\underline{E}^{(1)} = a^{(0,0)}\underline{P} - a^{(1,1)}\underline{P}^{(1)} \tag{A8}$$

$L^{(0,0)}$ and $L^{(1,1)}$ are called phenomenological coefficients, whereas $a^{(00)}$ and $a^{(11)}$ state coefficients. We report the physical meaning to them associated:

$a^{(00)}$ and $a^{(11)}$ reciprocal dielectric constants.
$L^{(00)}$ resistance.
$L^{(11)}$ conductivity.

It can be shown that it is possible to obtain the so called dielectric relaxation equation [10,34–36]:

$$\chi_{EP}^{(0)}\underline{E}+\frac{d\underline{E}}{dt}=\chi_{PE}^{(0)}\underline{P}+\chi_{PE}^{(1)}\frac{d\underline{P}}{dt}+\chi_{PE}^{(2)}\frac{d^2\underline{P}}{dt^2} \tag{A9}$$

where:

$$\chi_{EP}^{(0)}=a^{(1,1)}L^{(1,1)} \tag{A10}$$

$$\chi_{PE}^{(0)}=a^{(0,0)}\left(a^{(1,1)}-a^{(0,0)}\right)L^{(1,1)} \tag{A11}$$

$$\chi_{PE}^{(1)}=a^{(0,0)}\left(1+L^{(0,1)}-L^{(1,0)}\right)+a^{(1,1)}\left(L^{(0,0)}L^{(1,1)}-L^{(0,1)}L^{(1,0)}\right) \tag{A12}$$

$$\chi_{PE}^{(2)}=L^{(0,0)} \tag{A13}$$

If we perturb the medium with a polarization.

$$P=P_0\sin\omega t \tag{A14}$$

and by introducing some appropriate approximations, in the contest of linear response theory, phenomenological and state coefficients can be expressed as functions of the frequency as follows:

$$a^{(0,0)}(\omega)=\Gamma_1+\frac{\Gamma_2^{(1)}}{\omega\sigma} \tag{A15}$$

$$a^{(1,1)}(\omega)=\frac{\left[\Gamma_2^{(1)}+\Gamma_1\omega\sigma\right]^2}{\omega\sigma\Gamma_2^{(1)}\left(1+\omega^2\sigma^2\right)} \tag{A16}$$

$$L^{(1,1)}(\omega)=\frac{\omega\Gamma_2^{(1)}\left(1+\omega^2\sigma^2\right)}{\left[\Gamma_2^{(1)}+\Gamma_1\omega\sigma\right]^2} \tag{A17}$$

$$L^{(0,0)}(\omega)=\frac{\Gamma_{2R}}{\omega} \tag{A18}$$

where:

$$\Gamma_1=\frac{\varepsilon_1-\varepsilon_0}{\left(\varepsilon_1-\varepsilon_0\right)^2+\varepsilon_2^2} \tag{A19}$$

$$\Gamma_2=\frac{\varepsilon_2}{\left(\varepsilon_1-\varepsilon_0\right)^2+\varepsilon_2^2} \tag{A20}$$

and Γ_{2R} is the relaxed value for ω_R. Here ω_R is the frequency under which Γ_2 is almost constant [37]. Here ε_1 and ε_2 are real and imaginary part, respectively, of the complex dielectric constant and σ is the relaxation time. Here, we introduced a new quantity defined as:

$$\Gamma_2^{(1)}=\Gamma_2-\omega L^{(0,0)} \tag{A21}$$

$$P^{(0)}=\frac{\Gamma_1 P}{a^{(0,0)}} \tag{A22}$$

$$P^{(1)} = P - P^{(0)} = P\left(1 - \frac{\Gamma_1 P}{a^{(0,0)}}\right) \tag{A23}$$

The entropy production in the case of only dielectric relaxation phenomena becomes [8,26–28]:

$$\sigma^{(s)} = \frac{P_0^2}{T}\left(\omega L^{(0,0)} + \frac{\Gamma_2^{(1)}}{\left(1+\omega^2\sigma^2\right)}\right)\omega\cos^2\omega t \tag{A24}$$

where heat flow and density of electric current have been neglected.

References

1. Haussmann, H.J. Smoking and lung cancer: Future research directions. *Int. J. Toxicol.* **2007**, *26*, 353–364.
2. Jemal, A.; Bray, F.; Center, M.M.; Ferlay, J.; Ward, E.; Forman, D. Global cancer statistics. *CA Cancer J. Clin*. **2011**, *61*,69–90.
3. Scala, A.; Ficarra, S.; Russo, A.; Barreca, D.; Giunta, E.; Galtieri, A.; Grassi, G.; Tellone, E. A new erythrocyte-based biochemical approach to predict the antiproliferative effects of heterocyclic scaffolds: The case of indolone. *Biochim Biophys. Acta* **2015**, *1850*, 73–79.
4. Scala, A.; Ficarra, S.; Russo, A.; Barreca, D.; Giunta, E.; Galtieri, A.; Grassi, G.; Tellone, E. Alterations in Red Blood Cell Functionality Induced by an Indole Scaffold Containing a Y-Iminodiketo Moiety: Potential Antiproliferative Conditions. *Oxidative Med. Cell. Longev.* **2016**, *2016*, 1–11, doi:10.1155/2016/2104247.
5. Kim, T.; Oh, J.; Kim, B.; Lee, J.; Jeon, S. A study of dielectric properties of fatty, malignant and fibro-glandular tissues in female human breast. In Proceedings of the 2008 Asia-Pacific Symposium on Electromagnetic Compatibility and 19th International Zurich Symposium on Electromagnetic Compatibility, Singapore, 19–23 May 2008; pp. 216–219.
6. O'Rourke, A.P.; Lazebnik, M.; Bertram, J.M.; Converse, M.C.; Hagness, S.C.; Webster, J.G.; Mahvi, D.M. Dielectric properties of human normal, malignant and cirrhotic liver tissue: in vivo and ex vivo measurements from 0.5 to 20 GHz using a precision open ended coaxial probe. *Phys. Med. Biol.* **2007**, *52*, 4707–4719.
7. Wang, J.R.; Sun, B.Y.; Wang, H.X.; Pang, S.; Xu, X.; Sun, Q. Experimental Study of Dielectric Properties of Human Lung Tissue in Vitro. *J. Med. Biol. Eng.* **2014**, *34*, 598–604.
8. Chen, X.; Lv, X.; Wang, H. Lung carcinoma recognition by blood dielectric spectroscopy *Bio Med. Mater. Eng.* **2015**, *26*, S895–S901.
9. Farsaci, F.; Tellone, E.; Cavallaro, M.; Russo, A.; Ficarra, S. Low frequency dielectric characteristics of human blood: a non-equilibrium thermodynamic approach. *J. Mol. Liq.* **2013**, *188*, 113–119.
10. Farsaci, F.; Ficarra, S.; Russo, A.; Galtieri, A.; Tellone, E. Dielectric properties of human diabetic blood: thermodynamic characterization and new prospective for alternative diagnostic techniques. *J. Adv. Dielectr.* **2015**, *5*, 1550021, doi:10.1142/s2010135x15500216.
11. Farsaci, F.; Russo, A.; Ficarra, S.; Tellone, E. Dielectric properties of human normal and malignant liver tissue: a non-equilibrium thermodynamics approach. *Open Access Libr. J.* **2015**, *2*,1395.
12. Farsaci, F.; Ficarra, S.; Russo, A.; Galtieri, A.; Tellone, E. On evaluation of electric conductivity by mean of non-equilibrium thermodynamic approach with internal variables. An application to human erythrocyte suspension for metabolic characterizations. *J. Mol. Liq.* **2016**, *224*, 1181–1188.
13. Farsaci, F.; Tellone, E.; Galtieri, A.; Russo, A.; Ficarra, S.; Evaluation of the human blood entropy production: a new thermodynamic approach. *J. Ultrasound* **2016**, *19*, 265–273.
14. Farsaci, F.; Tellone, E.; Russo, A.; Galtieri, A.; Ficarra, S. Rheological properties of human blood in the network of non-equilibrium thermodynamic with internal variables by means of ultrasound wave perturbation. *J. Mol. Liq.* **2017**, *231*, 206–212.
15. Farsaci, F.; Ficarra, S.; Galtieri, A.; Tellone, E. New non-equilibrium thermodynamic fractional visco-inelastic model to predict experimentally inaccessible processes and investigate pathophysiological cellular structures. *Fluids* **2017**, *2*, 59.
16. Farsaci, F.; Tellone, E.; Galtieri, A.; Ficarra, S. Molecular characterization of a peculiar blood clot fluidification by theoretical thermodynamic models and entropy production study. *J. Mol. Liq.* **2018**, *265*, 457–462.

17. Farsaci, F.; Tellone, E.; Galtieri, A.; Ficarra, S. Expanding the repertoire of dielectric fractional models: a comprehensive development and functional applications to predict metabolic alterations in experimentally-inaccessible cells or tissues. *Fluids* **2018**, *3*, 9.
18. Farsaci, F.; Tellone, E.; Galtieri, A.; Ficarra, S. Is a dangerous blood clot formation a reversible process? Introduction of new characteristic parameter for thermodynamic clot blood characterization: possible molecular mechanisms and pathophysiologic applications. *J. Mol. Liq.* **2018**, *262*, 345–353.
19. Farsaci, F.; Tellone, E.; Galtieri, A.; Ficarra, S. Electromagnetic waves propagation in normal and pathological hemoglobins: Thermodynamic comparative study of the influence of the relative macromolecular variability. *J. Mol. Liq.* **2019**, *291*, 111319.
20. Farsaci, F.; Tellone, E.; Galtieri, A.; Ficarra, S. A new model for thermodynamic characterization of hemoglobin. *Fluids* **2019**, *4*, 135.
21. Farsaci, F.; Tellone, E.; Galtieri, A.; Ficarra, S. Phenomenological approach on electromagnetic waves propagation in normal and diabetic blood, influence of the relative macromolecular structures. *J. Mol. Liq.* **2019**, *274*, 577–583.
22. Farsaci, F.; Tellone, E.; Galtieri, A.; Ficarra, S. A new model with internal variables for theoretical thermodynamic characterization of hemoglobin: Entropy determination and comparative study. *J. Mol. Liq.* **2019**, *279*, 632–639.
23. Farsaci, F., Tellone, E., Galtieri, A.; Ficarra, S. A thermodynamic characterization of the phenomena evolving in cancer pathology by dielectric relaxation in blood: A new approach by construction of TTM (Thermodynamic Tumor Matrix). *J. Mol. Liq.* **2020**, 113839, doi:10.1016/j.molliq.2020.113839.
24. Gabriel, S.; Lau R.W.; Gabriel, C. The dielectric properties of biological tissues: III. Parametric models for the dielectric spectrum of tissues. *Phys. Med. Biol.* **1996**, *41*, 2271–2293.
25. Bellorofonte, C.; Vedruccio, C.; Tombolini, P.; et al. A non invasive detection of prostate cancer by electromagnetic interaction. *Eur. Urol.* **2005**, *47*, 29–37.
26. Sugitani, T.; Kubota, S.-I.; Kuroki, S.-I.; Sogo, K.; Arihiro, K.; Okada, M.; Kadoya, T.; Hide, M.; Oda, M.; Kikkawa, T. Complex permittivities of breast tumor tissues obtained from cancer surgeries. *Appl. Phys. Lett.* **2014**, *104*, 253702.
27. Joines, W.T.; Zhang, Y.; Li, C.; Jirtle, R.L. The measured electrical properties of normal and malignant human tissues from 50 to 900 MHz. *Med. Phys.* **1994**, *21*, 547–550.
28. Foster, K.R.; Schepps, J.L. Dielectric properties of tumor and normal tissues at radio through microwavefrequencies. *J. Micro. Power.* **1981**, *16*, 107–119.
29. Sha, L. Ward, E.R. Story, B. A review of dielectric properties of normal and malignant breast tissue. In Proceedings of the IEEE SoutheastCon, Columbia, SC, USA, 5–7 April 2002; pp. 457–462
30. Redmann, K.; Müller, V.; Tanneberger, S.; Kalkoff,W. The membrane potential of primary ovarian tumor cells in vitro and its dependence on the cell cycle. *Acta Biol. Med. Ger.* **1972**, *28*, 853.
31. Lobikin, M.; Chernet, B.; Lobo, D.; Levin, M. Resting potential, oncogene-induced tumorigenesis, and metastasis: the bioelectric basis of cancer in vivo. *Phys. Biol*. **2012**, *9*, 065002.
32. Warburg, O. On respiratory impairment in cancer cells. *Science* **1956**, *124*, 269–270.
33. Hay, N. Reprogramming glucose metabolism in cancer: can it be exploited for cancer therapy? *Nat. Rev. Cancer* **2016**, *16*, 635–649.
34. Kluitenberg, G.A. On dielectric and magnetic relaxation phenomena and non-equilibrium thermodynamics. *Physica* **1973**, *68*, 75–82.
35. Kluitenberg, G.A. On dielectric and magnetic relaxation phenomena and vectorial internal degrees of freedom in thermodynamics.*Phys. A Stat. Mech. Appl.* **1977**, *87*, 302–330.
36. Kluitenberg, G.A. On vectorial internal variables and dielectric and magnetic relaxation phenomena. *Phys. A Stat. Mech. Appl*. **1981**, *109*, 91–122.
37. McCrum, N.G.; Read, B.E.; Williams, G. *An Elastic and Dielectric Effects in Polymeric Solids*; John Wiley and Sons Ltd.: London, UK, 1967.